



## DSC study of biodegradable poly(lactic acid) and poly(hydroxy ester ether) blends<sup>☆</sup>

X. Cao<sup>a</sup>, A. Mohamed<sup>b</sup>, S.H. Gordon<sup>c</sup>, J.L. Willett<sup>c,\*</sup>, D.J. Sessa<sup>c</sup>

<sup>a</sup> Department of Chemistry, Bradley University, 1815 N. University Street, Peoria, IL 61614, USA

<sup>b</sup> Cereal Products and Food Science Research Unit, USDA, Agricultural Research Service, 1815 N. University Street, Peoria, IL 61614, USA

<sup>c</sup> Plant Polymer Research Unit, National Center for Agriculture Utilization Research, USDA, Agricultural Research Service, 1815 N. University Street, Peoria, IL 61614, USA

Received 5 November 2001; received in revised form 8 April 2003; accepted 8 April 2003

### Abstract

DSC heating–cooling cycles (0–200 °C) were repeated on poly(lactic acid)/poly(hydroxy ester ether) (PLA/PHEE) blends to study the miscibility of the two polymers. Initial thermograms show two distinguishable  $T_g$  values corresponding to the respective neat polymers, accompanied by a crystallization and a melting peak for the PLA. Subsequent DSC runs show that the thermogram profiles depend on the number of heating–cooling cycles the blends are subjected to. As the number of cycles increases,  $T_{g,PLA}$  and  $T_{g,PHEE}$  shift toward each other and eventually merge into a single  $T_g$ , while  $\Delta H_c$  and  $\Delta H_m$  of PLA increase to maximum values then decrease to zero. It is concluded that after repeated heating–cooling cycles, PLA and PHEE achieve mixing on a molecular level, i.e. PLA and PHEE are miscible. The number of cycles needed to reach a single  $T_g$ , maximum  $\Delta H$  and zero  $\Delta H$ , are dependent on blend composition.

Published by Elsevier B.V.

**Keywords:** PLA; PHEE; Blends; Miscibility; Thermal properties

### 1. Introduction

The use of non-renewable, petroleum-based chemicals for the synthesis and manufacture of commodity polymers, and the environmental concerns generated by their disposal, pose major challenges to the polymer industry. The main strategies to address these problems are to utilize polymeric materials from

renewable sources, and to develop biodegradable polymeric materials.

One of the most abundant polymeric materials from renewable resources is starch. While abundant and inexpensive, however, starch alone as a material does not offer satisfactory properties for many applications. Meanwhile, the few synthetic biodegradable polymers with satisfactory properties are prohibitively expensive when compared to commodity non-biodegradable polymers. A common approach is to make blends/composites of starch and other biodegradable synthetic polymers to produce materials of satisfactory properties and a low overall cost.

Three-component blends of cornstarch, poly(lactic acid) (PLA), and poly(hydroxy ester ether) (PHEE), have been prepared with satisfactory properties and

<sup>☆</sup> Names are necessary to report factually on available data; however, the USDA neither guarantees nor warrants the standard of the product, and the use of the name by USDA implies no approval of the product to the exclusion of others that may also be suitable.

\* Corresponding author. Tel.: +1-309-681-6556;

fax: +1-309-681-6691.

E-mail address: [willetjl@ncaur.usda.gov](mailto:willetjl@ncaur.usda.gov) (J.L. Willett).

processibility [1,2]. Of the three biodegradable components, starch is used to reduce the overall cost, PLA provides thermal and mechanical properties, while PHEE acts as a processing aid and increases inter-component interactions.

Recent FTIR results demonstrate hydrogen bonding between PLA carbonyls and PHEE hydroxyls [3]. Since inter-component hydrogen bonding often results in polymers being miscible or semi-miscible, DSC experiments were performed to characterize PLA/PHEE blends, focusing on the miscibility of these two polymers. As part of the experiment, a novel DSC procedure was devised to examine the material.

## 2. Experimental

### 2.1. Materials

Pelletized PHEE was supplied by the Dow Chemical Company (Midland, MI) with a weight average molecular weight of  $6.7 \times 10^4$  g/mol [4]. Pelletized PLA was supplied by the Cargill Dow LLC (Minnetonka, MN) with a molecular weight  $M_W = 2 \times 10^5$  g/mol.

### 2.2. Blend preparations

Blends were prepared using a Brabender (South Hackensack, NJ) batch mixer. The mixing temperature was 190 °C, and the mixer was torque calibrated before sample addition. PLA and PHEE pellets (total sample weight 50.0 g) were added to the mixing chamber with the mixing screw speed set at 0.17 Hz. After mixing for 5 min at 0.17 Hz, the screw speed was increased to 0.83 Hz for 10 min, resulting in a total mixing time of 15 min. PLA/PHEE blends of different composition, i.e. different  $W_{\text{PLA}}/W_{\text{PHEE}}$  ratio, were prepared by using the appropriate amounts of the two polymers. In addition, neat PLA and PHEE were also processed using the same procedure and used as controls in the thermal experiments.

Specific mechanical energy (SME) of the mixing process was calculated based on the total mechanical energy during the mixing. The SME values obtained for PLA/PHEE blends of different compositions ranged from 0.1 to 1.3 kJ/kg. Increasing PHEE content in the blend resulted in lower SME values due to

PHEE's low melt viscosity. These SME values are on the same order of magnitude as the SME values obtained from typical blending procedures using single- or twin-screw extruders.

### 2.3. DSC measurements

PLA/PHEE blends were pulverized using liquid nitrogen in a sealed stainless steel vial containing a stainless steel ball bearing for up to 5 min on a Wig-L-Bug amalgamator (Crescent Dental Manufacturing, Lyons, IL). The powdered sample, about 50 mg in weight, was packed into a stainless steel high volume DSC pan and sealed. DSC measurements were carried out using a TA Instruments (New Castle, DE) DSC 2920 calibrated at 10 °C/min ramp speed with indium. For repeated heating-cooling cycling measurements, the following thermal procedure was used: isotherm at 0 °C for 1 min, ramp 10 °C/min from 0 to 200 °C, isotherm at 200 °C for 1 min, and ramp 10 °C/min from 200 to 0 °C. The procedure was repeated until the experiment was finished. Before and after sample weights were found to be identical.

TGA measurements were made using a TA Instruments TGA 2050. A 10–20 mg sample was spread out on a platinum pan. Both isothermal (200 °C) and non-isothermal (ramp 10 °C/min) measurements were carried out.

## 3. Results and discussion

### 3.1. DSC thermograms

As a semi-crystalline polymer under the measurement conditions specified as above, PLA's thermogram (second heating) consists of a glass transition, crystallization exotherm and melting endotherm peaks (Fig. 1). The glass transition temperature,  $T_{g,\text{PLA}}$ , is found to be 61.8 °C, and the specific heat capacity  $\Delta C_{p,\text{PLA}} = 0.51$  J/(g °C). These values compare well with  $T_g = 61$  °C and  $\Delta C_p \sim 0.55$  J/(g °C) as reported by Witzke [5]. As evident by the flat heat flow in the cooling portion of the thermogram, the PLA sample does not crystallize during cooling at 10 °C/min ramp. Instead, the sample crystallizes during heating, as indicated by the exotherm in the heating portion of the DSC thermogram. The crystallization occurs

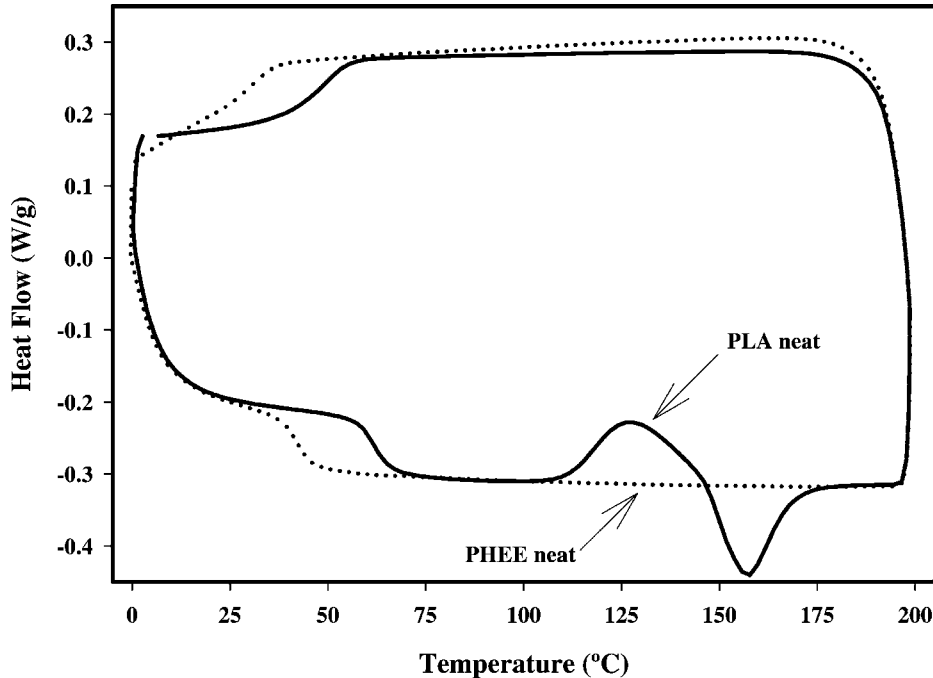


Fig. 1. DSC thermograms (second heating–cooling) of the semi-crystalline PLA, which consists of a glass transition ( $T_{g,PLA} = 61.8^{\circ}\text{C}$ ), crystallization exotherm (peak temperature  $T_c = 127^{\circ}\text{C}$ ) and melting endotherm (peak temperature  $T_m = 157^{\circ}\text{C}$ ); and the amorphous PHEE, which consists of a glass transition ( $T_{g,PHEE} = 41.3^{\circ}\text{C}$ ).

between 111 and  $147^{\circ}\text{C}$ , with peak temperature at  $T_c = 127^{\circ}\text{C}$ . The crystallization enthalpy,  $\Delta H_c$ , is calculated to be  $\Delta H_c = -10.9\text{J/g}$ , based on the exotherm heat flow. The degree of crystallinity  $X_c$  is calculated to be  $X_c = \Delta H_c/93 = 11.7\%$ , using  $93\text{J/g}$  as the melting enthalpy of a PLA crystal of infinite size [6]. Melting of this regained crystallinity follows immediately, indicated by the endotherm with peak temperature  $T_m = 157^{\circ}\text{C}$  and melting enthalpy  $\Delta H_m = 11.0\text{J/g}$ . The fact that  $\Delta H_c + \Delta H_m \approx 0$  suggests that the PLA sample's thermal history has been erased by the first DSC heating–cooling cycle.

PHEE's DSC thermogram (second heating) displays a single glass transition (Fig. 1). The glass transition temperature,  $T_{g,PHEE}$ , is  $41.3^{\circ}\text{C}$ , in agreement with the  $T_g$  value reported by Mang et al. [7].  $\Delta C_{p,PHEE}$  is  $0.41\text{J}/(\text{g}^{\circ}\text{C})$ .

The DSC thermogram (second heating) of the 50/50 PLA/PHEE blend shows two distinguishable  $T_g$  values, and the PLA crystallization exotherm and melting endotherm (Fig. 2). The two  $T_g$  values are  $40.0$  and  $59.1^{\circ}\text{C}$ , respectively. The crystallization

exotherm has a peak temperature  $T_c = 121^{\circ}\text{C}$ , enthalpy  $\Delta H_c = -14.5\text{J/g}$ . The melting endotherm has a peak temperature  $T_m = 156^{\circ}\text{C}$ , and enthalpy  $\Delta H_m = 17.4\text{J/g}$ . The two  $T_g$  values correspond well with the  $T_g$  values of the two neat polymers, while the  $T_c$  and  $T_m$  values correspond well with PLA's  $T_c$  and  $T_m$  values. This suggests that the two components in the blend respond to the heating–cooling independently, i.e. the two polymers are not miscible.

FTIR analysis of the same PLA/PHEE blends, however, indicates hydrogen bonding between PLA carbonyls and PHEE hydroxyls [3]. This suggests that the two polymers should have certain degree of miscibility, since polymer pairs with specific interactions are generally found to be miscible or semi-miscible. The FTIR results also show that only a few percent of PLA carbonyls participate in hydrogen bonding with PHEE. Such a small level of interaction may not be enough to significantly influence the blend's thermal properties such as glass transition and crystallization, consistent with the DSC results as shown in Fig. 2.

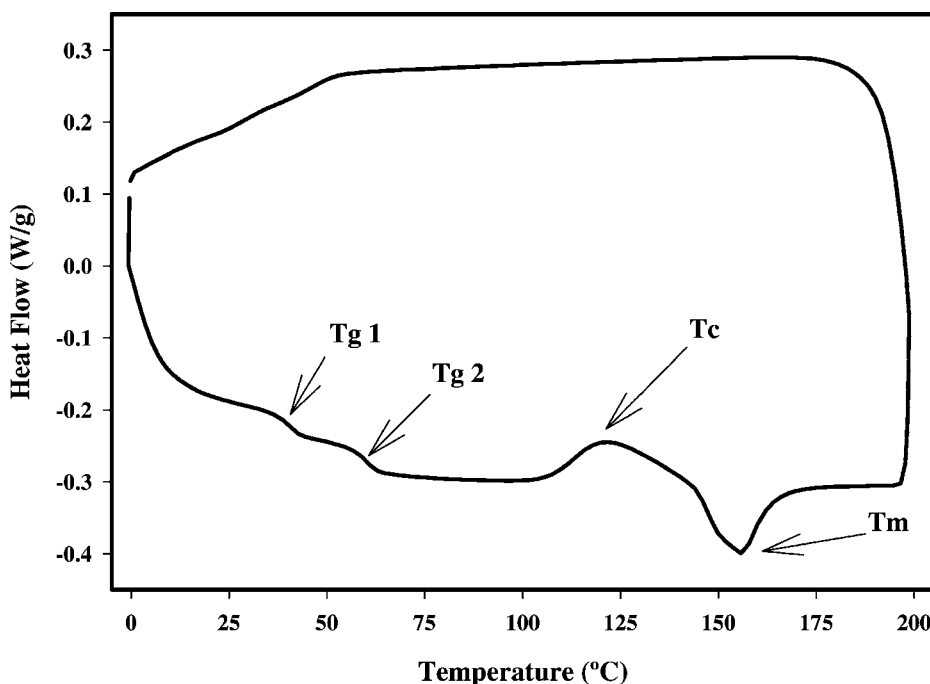


Fig. 2. DSC thermogram (second heating–cooling) of the 50/50 PLA/PHEE blend consists of two distinguishable  $T_g$  values:  $T_{g,1} = 40.0^\circ\text{C}$ ,  $T_{g,2} = 59.1^\circ\text{C}$ , a crystallization exotherm  $T_c = 121^\circ\text{C}$  and a melting endotherm  $T_m = 156^\circ\text{C}$ .

The blends as obtained from the mixing bowl are phase separated. In a phase separated system, interactions can only occur at the interfacial regions, therefore only a small portion of polymers are participating in the interaction. To provide longer mixing times by inter-diffusion, a DSC heating–cooling ( $0\text{--}200^\circ\text{C}$ ) cycling procedure, as described in Section 2.3, was devised and applied to the blends. For each heating–cooling cycle, the blend was at a temperature above the  $T_g$  values for 29 min, and was at a temperature above PLA's  $T_m$  for 9 min.

The DSC thermograms of the 50/50 PLA/PHEE blend at three representative stages of this heating–cooling procedure are shown in Fig. 3. When compared to Fig. 2, the thermogram of the same blend at the second heating–cooling cycle, it is apparent that the repeated DSC heating–cooling cycling has a significant effect on the blend's thermal properties. The two  $T_g$  values change as a function of number DSC cycles and eventually merge into a single  $T_g$ .  $\Delta H_c$  and  $\Delta H_m$  decrease with the number of DSC cycles and eventually reach zero.

### 3.2. Glass transition

Fig. 4 shows three sets of  $T_g$  values of three PLA/PHEE blends as function of DSC cycles. Of these three  $T_g$  sets, and of all the other  $T_g$  sets for PLA/PHEE blends of different compositions, the common feature is that at the start of DSC cycling measurement, two  $T_g$  values are distinguishable, corresponding to the neat polymers. As the number of DSC cycles increases, the two  $T_g$  values approach each other, i.e.  $T_{g,PLA}$  decreases while  $T_{g,PHEE}$  increases. After a number of heating–cooling cycles, the two  $T_g$  values merge into a combined, single  $T_g$  ( $T_{g,com}$ ) and afterwards only a single  $T_g$  is seen.

In addition, there is a significant difference in the manner in which the two  $T_g$  values merge. For blends with high PLA content, such as the 90/10 blend shown in Fig. 4A, it is as if that  $T_{g,PHEE}$  disappears at the point where the two  $T_g$  values merge, and  $T_{g,com}$  subsequently behaves as a continuation of  $T_{g,PLA}$ . For blends of intermediate PLA content, such as the 75/25 blend shown in Fig. 4B, both  $T_{g,PLA}$  and  $T_{g,PHEE}$  seem

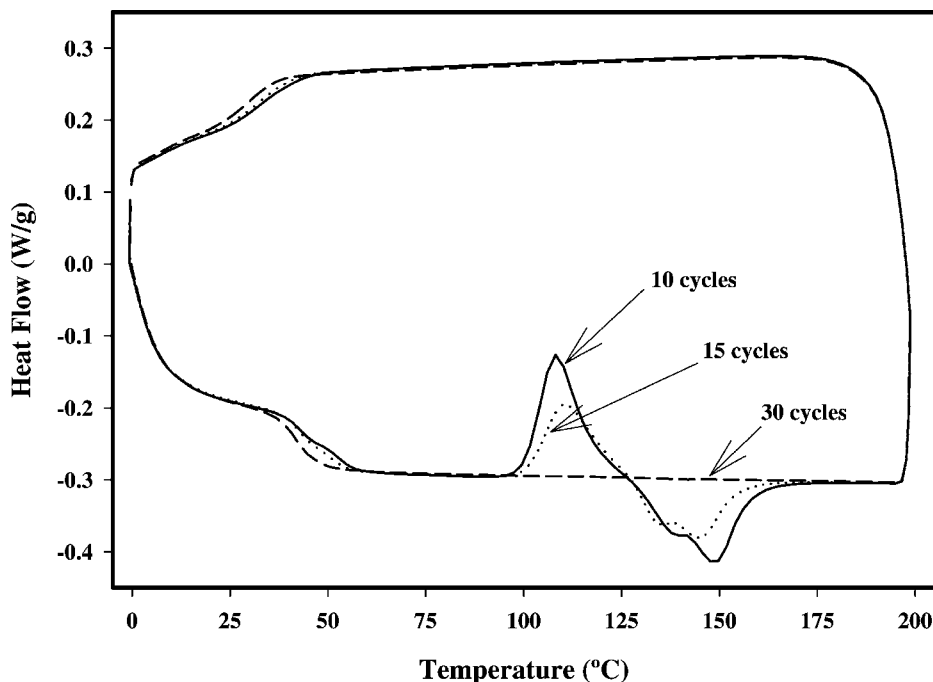


Fig. 3. The DSC thermograms of the 50/50 PLA/PHEE blend at three different DSC heating-cooling cycles (cycles 10, 15 and 30).

to disappear at the same time (cycle), and  $T_{g,com}$  appears to be the average of  $T_{g,PLA}$  and  $T_{g,PHEE}$ . For blends of low PLA content, such as the 40/60 blend shown in Fig. 4C, it is as if that  $T_{g,PLA}$  disappears at the point where the two  $T_g$  values merge, and  $T_{g,com}$  afterwards behaves just as a continuation of  $T_{g,PHEE}$ .

The glass transition in a polymer blend depends on the extent of miscibility of the two components. For substantially total immiscibility, i.e. total phase separation, two glass transitions will be observed at the glass transitions of the neat polymers. Usually, however, at least some mixing is observed at the polymer-polymer interface, resulting in an inward shifting of the two glass transitions. In the case where there is extensive but incomplete mixing, i.e. partial miscibility, the inward shift of the two  $T_g$  values is a function of the size of the phase domains, the shift increases as the domain size decreases. Even greater miscibility yields one broad transition, which narrows (to 20–30 °C temperature range) for thermodynamic miscibility.

As shown in Figs. 3 and 4, at the beginning of DSC cycling, two distinguishable  $T_g$  values corresponding to the glass transitions of the two neat polymers are ob-

served, indicating total phase separation. As the number of DSC cycles increases, the two  $T_g$  values shift inward, suggesting that the phase domains decrease and the extent of mixing increases. After some number of DSC cycles, e.g. more than 40 cycles in the case of the 75/25 blend (Fig. 4B), the two  $T_g$  values merge into a single  $T_{g,com}$  which eventually narrows to a sharp transition range (onset 43 °C, endpoint 55 °C), suggesting a great extent of mixing and miscibility or even thermodynamic miscibility.

The three types of  $T_g$  merging, as demonstrated in Fig. 4, can be explained as follows. In the initial stages of the DSC cycling procedure, PHEE is dispersed in the continuous PLA matrix in blends with high PLA contents. As the number of cycles increases, the PHEE domains decrease in size as PHEE diffuses into PLA. This would give rise to the type of  $T_g$  behavior as shown in Fig. 4A. Our results show that blends with PLA contents  $\geq 80\%$  have such  $T_g$  behavior. In blends with low PLA contents, PLA phase domains are dispersed in the PHEE matrix at the early DSC cycling stage. Such a system will give rise to the type of  $T_g$  behavior as shown in Fig. 4C. Blends with PLA

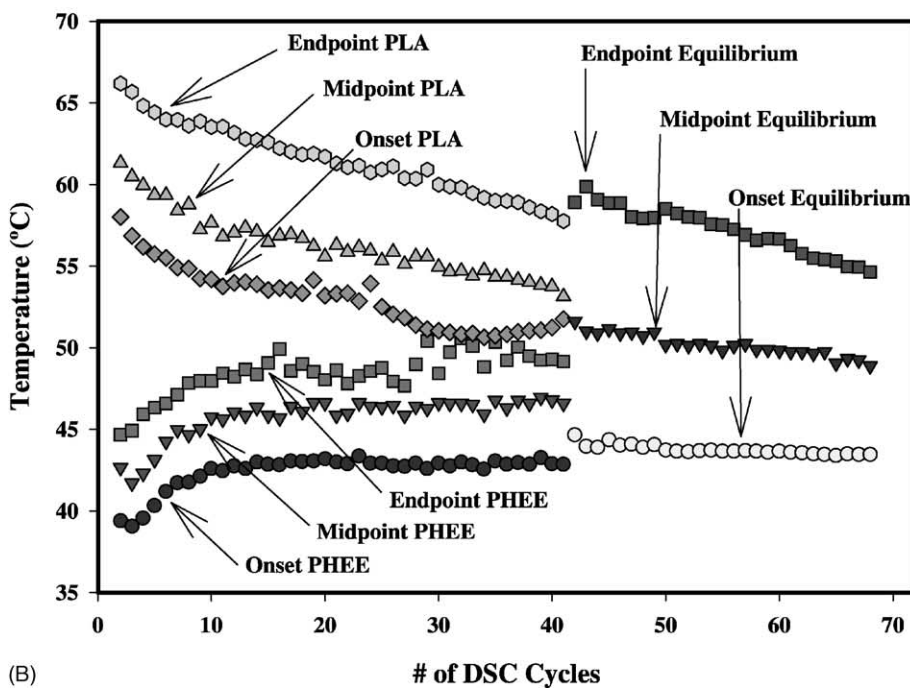
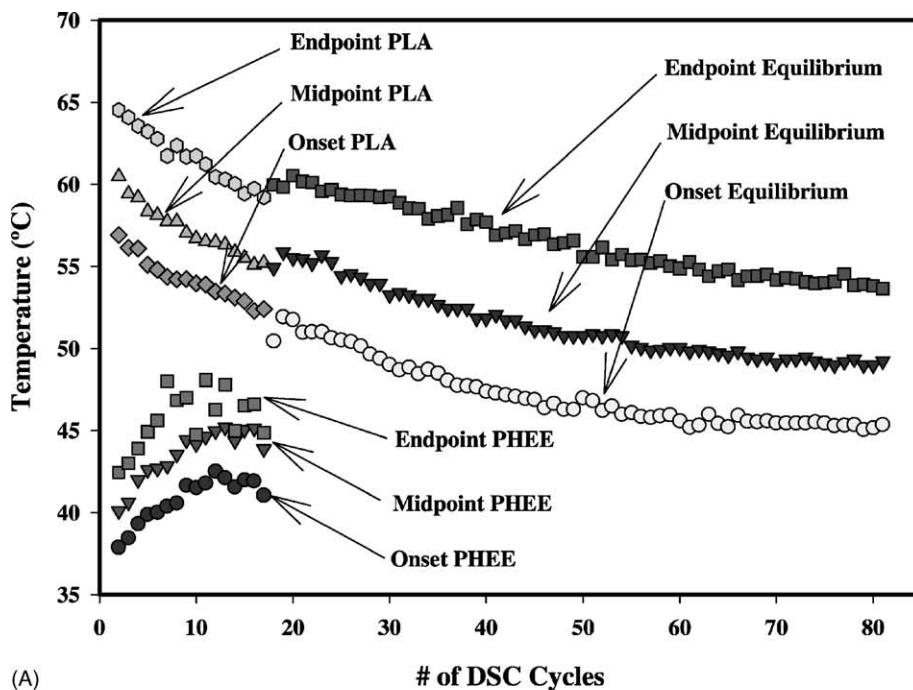


Fig. 4. (A)  $T_g$  values for the 90/10 PLA/PHEE blend. Before nine cycles, two  $T_g$  values are distinguishable, afterwards only a single  $T_g$  is seen. The onset, endpoint as well as  $T_g$  (midpoint) are plotted to show the breadth of the transition. (B)  $T_g$  values for the 75/25 PLA/PHEE blend. (C)  $T_g$  values for the 40/60 PLA/PHEE blend.

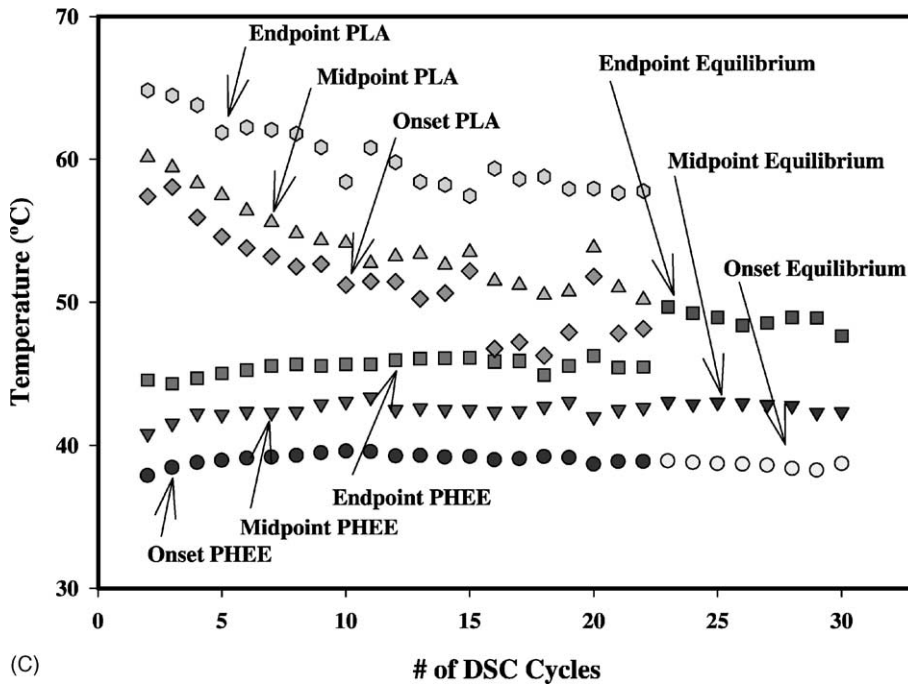


Fig. 4. (Continued).

contents  $\leq 50\%$  follow this pattern. For blends with intermediate PLA contents, PLA and PHEE domains are probably inter-dispersed before the thermal cycling procedure. As the number of cycles increases, both PLA and PHEE domains decrease in size and eventually diminish at about the same time (cycle), thus demonstrating behavior as shown in Fig. 4B. Blends with PLA contents  $50\% < \text{PLA}\% \leq 75\%$  are found to have such  $T_g$  patterns.

Fig. 5 shows the composition dependence of the blends' combined  $T_g$  values,  $T_{g,\text{com}}$ . The Gordon–Taylor equation (Eq. (1)) is frequently used to describe the composition dependence of the glass transition in polymer blends [8]:

$$T_g^b = \frac{W_1 T_{g,1} + k W_2 T_{g,2}}{W_1 + k W_2}, \quad (1)$$

where  $W_i$  and  $T_{g,i}$  refer to the weight fraction and the glass transition temperature, and 1, 2 and b denote the neat components and blend, respectively. The adjustable parameter  $k$  has been interpreted as a miscibility measure since it can be related to the interaction strength between the components in a blend.

When Eq. (1) is applied to the experimental results of PLA/PHEE blend, a value of  $k = 4.46$  is obtained with  $R^2 = 0.94$ . However, it has been pointed out that the value of this parameter cannot be used to compare two completely different blend series [9].

The Gordon–Taylor equation is often modified as:

$$T_g^b = \frac{W_1 T_{g,1} + k W_2 T_{g,2}}{W_1 + k W_2} + q W_1 W_2, \quad (2)$$

where the second term represents the effect of polymer–polymer interactions, e.g. hydrogen bonding [10]. When Eq. (2) is applied, a slightly better fit is found with  $k = 2.63$ ,  $q = -11.76$ ,  $R^2 = 0.97$ . The parameter  $q$  is a sum of contributions to polymer–polymer interaction by steric, electronic and polarization effects, and hydrogen bonding. In general, in polymer pairs where there is hydrogen bonding, as in PLA/PHEE blend, negative  $q$  values are attributed to contributions by electronic and/or steric/polarizability effects. For comparison, the prediction by the Fox equation (Eq. (3)) is also shown:

$$\frac{1}{T_g^b} = \frac{W_1}{T_g^1} + \frac{W_2}{T_g^2}. \quad (3)$$

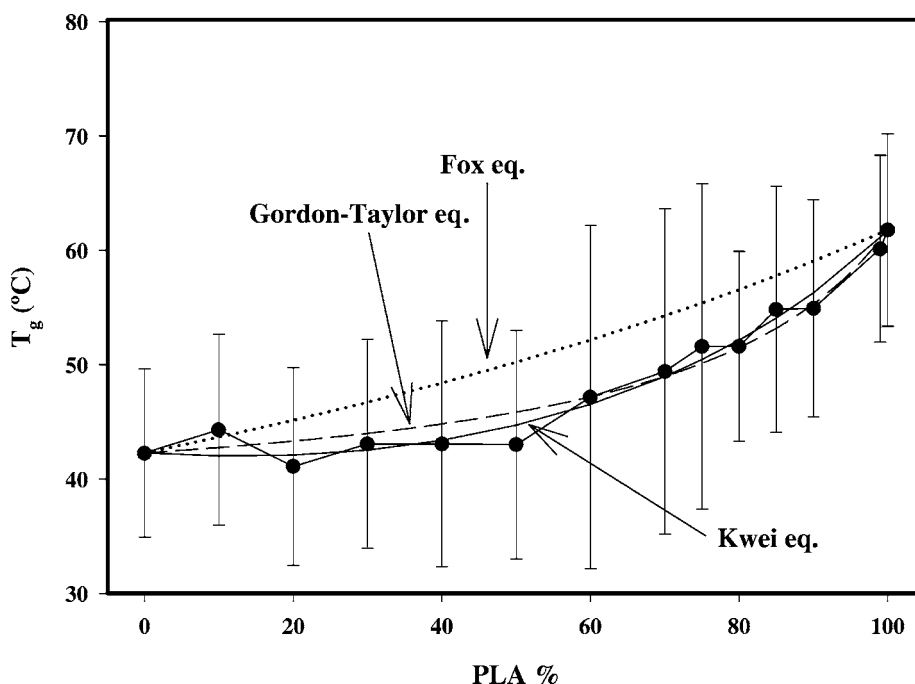


Fig. 5.  $T_g$  vs. composition in PLA/PHEE blends. The error bars represent the glass transition breadth ( $T_{\text{endpoint}} - T_{\text{onset}}$ ). The predicted  $T_g$  values by the Fox equation, the Gordon–Taylor equation with  $k = 4.46$ , and the Kwei equation with  $k = 2.63$  and  $q = -11.76$  are also shown.

### 3.3. Crystallization and melting

As mentioned earlier, the PLA in the blend recrystallizes during heating. The melting of this crystallinity follows immediately:  $T_m - T_c \approx 35^\circ\text{C}$ . Both the crystallization exotherm enthalpy  $\Delta H_c$  and the melting endotherm enthalpy  $\Delta H_m$  are dependent on the number of DSC cycles. Fig. 6 shows a typical plot of  $\Delta H_c$  and  $\Delta H_m$  as function of number of DSC cycles for the 50/50 PLA/PHEE blend.  $\Delta H_c$  and  $\Delta H_m$  are mirror images ( $\Delta H_{\text{total}} = \Delta H_c + \Delta H_m \approx 0\text{J/g}$ ), indicating that for each thermal cycle the crystallinity is completely melted and the blend has little residual crystallinity at the beginning or end of each DSC cycle. The magnitude of  $\Delta H_c$  increases from 14.5 J/g at cycle 2 ( $X_c = 15.6\%$ ), to a maximum of 28.9 J/g at cycle 6 ( $X_c = 31.1\%$ ), indicating the crystallinity increases as the number of cycles increases. After the maximum at cycle 6,  $\Delta H_c$  decreases as the number of cycles increases and eventually approaches zero:  $\Delta H_c < 0.2\text{J/g}$  at cycle 28 after which the experiment was stopped.

The behavior of  $\Delta H$  as a function of the number of thermal cycles is also dependent on blend composition. Fig. 7 shows representative  $\Delta H$  values as a function of the number of cycles for several blend compositions. The common feature is that as the number of thermal cycles increases, the crystallinity initially increases, reaches a maximum value, and then gradually decreases and eventually reaches zero. The general trend is that blends with higher PLA content require more cycles for the crystallinity to reach zero. However, it takes approximately the same number of cycles ( $5 \pm 2$ ) for  $\Delta H$  values of different blends to reach their respective maxima. The maximum values of  $\Delta H_c$  and  $\Delta H_m$  for different blends can be divided into two groups (Fig. 8): blends with PLA content  $\geq 50\%$ , where  $\Delta H_{\text{max}} \approx 30\text{J/g}$  and is independent of the blend's composition; and blends with PLA content  $\leq 40\%$ , where  $\Delta H_{\text{max}}$  decreases as PLA content decreases.

As pointed out earlier, at the beginning of DSC cycling procedure, the blends are phase separated: blends with PLA content  $\geq 50\%$  have PLA as



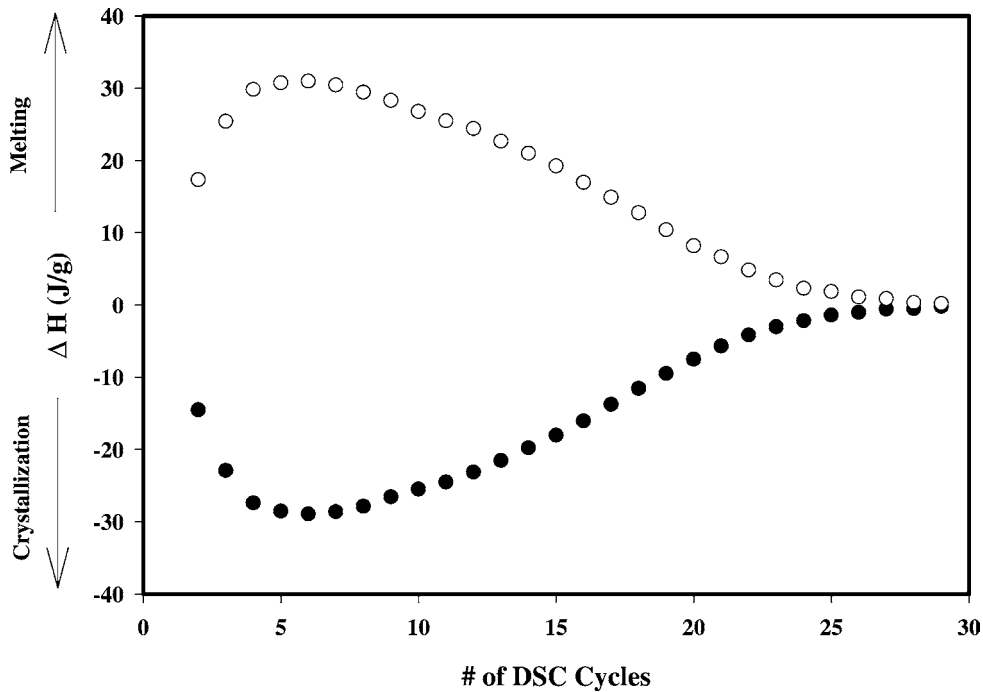


Fig. 6. Crystallization enthalpy  $\Delta H_c$  and melting enthalpy  $\Delta H_m$  as function of DSC cycles for the 50/50 PLA/PHEE blend. The enthalpies reach maximum values at cycle 6 and reach zero at cycle 28.

continuous phase (matrix) while blends with PLA content  $\leq 40\%$  have PLA as micro-phase domains dispersed in PHEE continuous matrix, and the PLA in either phase has relatively low  $\Delta H_c$ , similar to the neat PLA ( $X_c \sim 12\%$ ; Fig. 1). The repeated heating–cooling cycles could have opposing effects on PLA's crystallinity and thus on the  $\Delta H_c$  values of these blends. One effect is similar to that of annealing, consequently increasing  $\Delta H_c$  value. The other effect is to increase the phase mixing thus decreasing  $\Delta H_c$ , since more mixing hinders PLA's ability to recrystallize. Figs. 7 and 8 suggest that, for blends with PLA%  $\geq 50\%$ , where PLA phase is continuous, the annealing effect is dominant in the early DSC cycling process before the diffusional mixing takes over, and  $\Delta H_{max} \sim 30$  J/g is reached, comparable to that of the neat PLA ( $X_c \sim 32\%$ ). For blends with PLA contents  $\leq 40\%$  where PLA is the dispersed phase, the mixing effect dominates, and  $\Delta H_c$  value does not reach a maximum  $\Delta H_c$  of neat PLA before it starts to decrease.  $\Delta H_{max}$  values are composition dependent probably because the PLA domain size in

these blends is also composition dependent: the lower PLA content, the smaller the PLA phase domains, the faster they dissipate thus the smaller  $\Delta H_{max}$  values.

After an appropriate number of thermal cycles,  $\Delta H_c = 0$ , indicating PLA is no longer capable of crystallizing. In order for amorphous PHEE to hinder or prevent PLA crystallization, PLA and PHEE must be mixed on a molecular level. These enthalpy results suggest that PLA and PHEE are miscible. This is in good agreement with the same conclusion drawn based on the blend's  $T_g$  behavior.

An effective way to judge miscibility is by the blend's optical clarity. Unless the components have identical refractive indices, blends from immiscible components usually are cloudy or milk white in appearance. When the sample is transparent, then the phase domains, if any, are very small (compared to the wavelength of visible light) and the components are said to be miscible or semi-miscible. For PLA and PHEE,  $n_{PLA} = 1.41$  [11], and  $n_{PHEE} = 1.55$ . The refractive index of PHEE is estimated from the refractive index increment  $dn/dc$  of PHEE

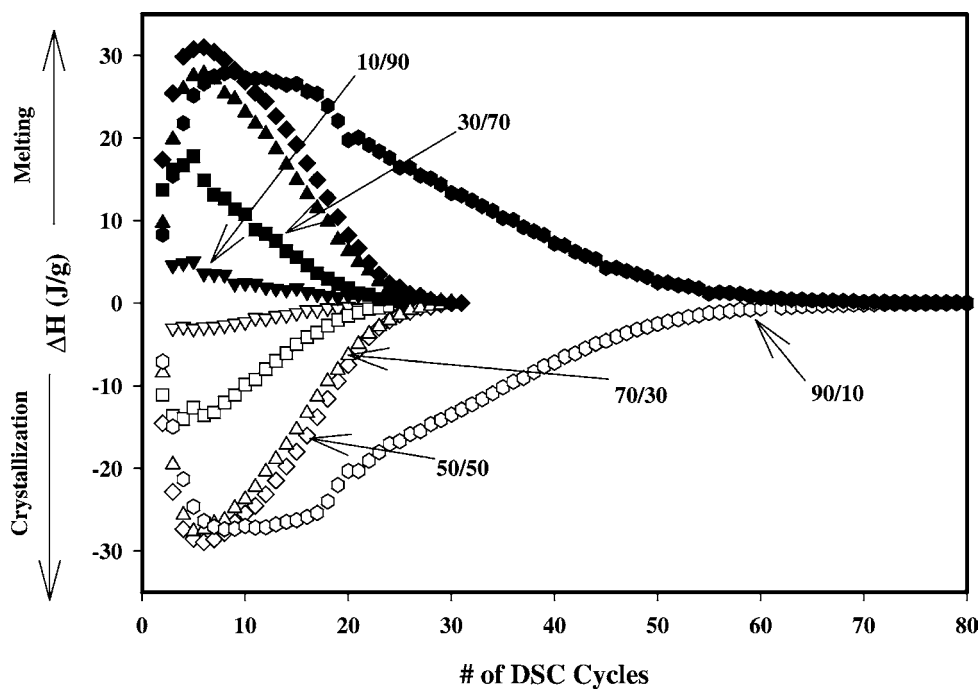


Fig. 7.  $\Delta H$  values of PLA in PLA/PHEE blends of different compositions at different DSC cycles. The initial increase in  $\Delta H$  indicates that the phase separated PLA is being annealed. The subsequent decrease indicates the micro-phase domains are being dissipated.

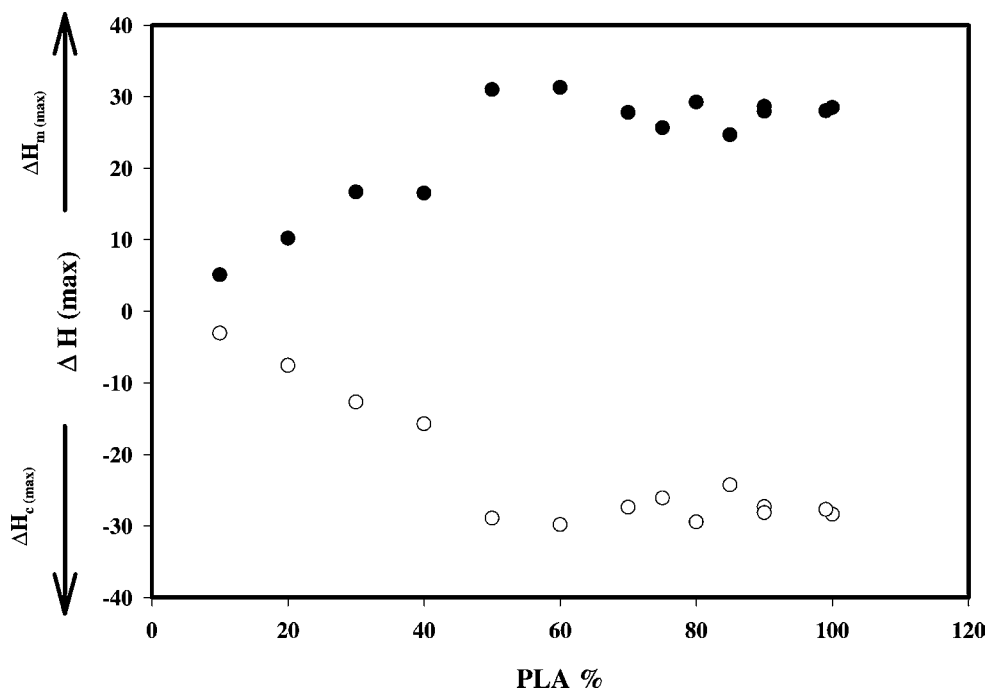


Fig. 8. Maximum  $\Delta H_c$  and  $\Delta H_m$  values as function of blends composition.

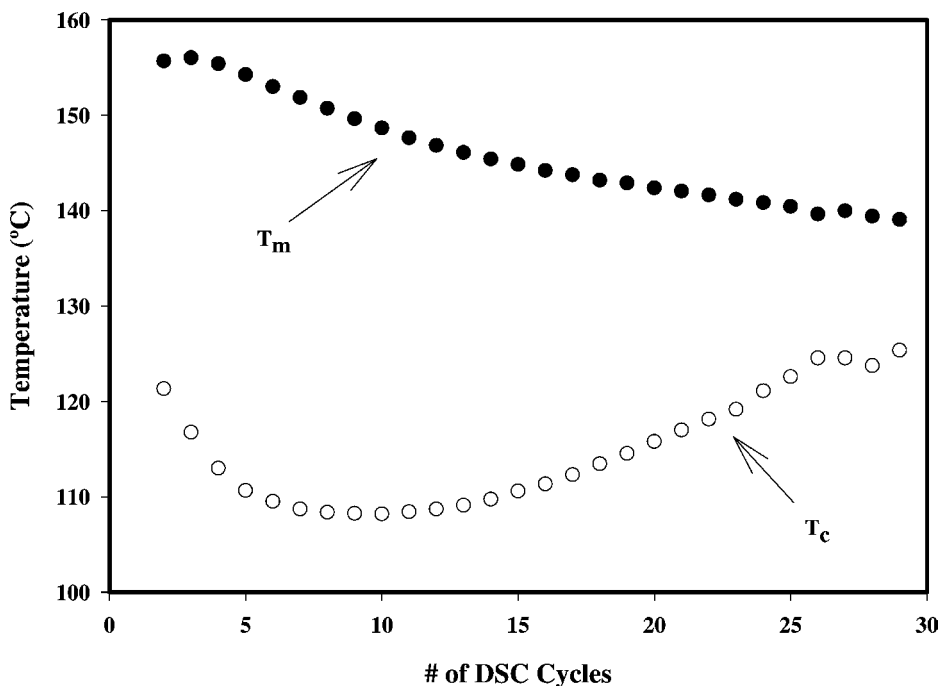


Fig. 9. Crystallization peak temperature  $T_c$  and melting peak temperature  $T_m$  as function of number of DSC cycles for the 50/50 PLA/PHEE blend.

in *N,N*-dimethylacetamide (DMAc) solution [4]. PLA/PHEE blends are milk white before DSC cycling procedures. However, the blends after the DSC cycling procedures are at least translucent. This observation suggests that PLA and PHEE are miscible.

Another feature of crystallization exotherm and melting endotherm is the crystallization temperature  $T_c$  and melting temperature  $T_m$ . Fig. 9 shows  $T_c$  and  $T_m$  for the 50/50 PLA/PHEE blend as a function of number of DSC cycles. As the cycling procedure progresses,  $T_c$  decreases initially to reach a minimum then increases, while  $T_m$  decreases monotonically. The physical nature behind this phenomenon is not clear, particularly the discrepancy between the  $T_c$  and  $T_m$  dependence on the number of cycles. Factors such as crystal size and type are probably involved. Further detailed studies by microscopic techniques are needed to explain the observed effects.

#### 3.4. TGA measurements

Fig. 10 shows the results of non-isothermal TGA measurements of the neat polymers and blends. Both

PLA and PHEE have thermal decomposition onset temperatures above 300 °C. The 50/50 PLA/PHEE blend's thermal decomposition onset temperature is approximately 280 °C. Fig. 11 shows the results of isothermal TGA measurements at 200 °C. The weight losses for the two neat polymers after holding at 200 °C for more than 300 min are not significant (<3%). The 50/50 blend, however, starts significant thermal decomposition after holding at 200 °C for about 1 h, and the total weight loss after 300 min is greater than 20%. These TGA results indicate that the DSC cycling procedure used in the experiment did not cause the samples (i.e. PLA and PHEE neat polymers and PLA/PHEE blends) to decompose significantly, which is in good agreement with the observation that the sample weights before and after the DSC procedure are identical.

The blend is less stable than the neat polymers. A 50/50 physical mixture of PLA and PHEE shows thermal properties that compare well to the calculated decomposition curves using data for the neat polymers. This difference between the blend and the physical mixture suggests that the blend, after melt processing

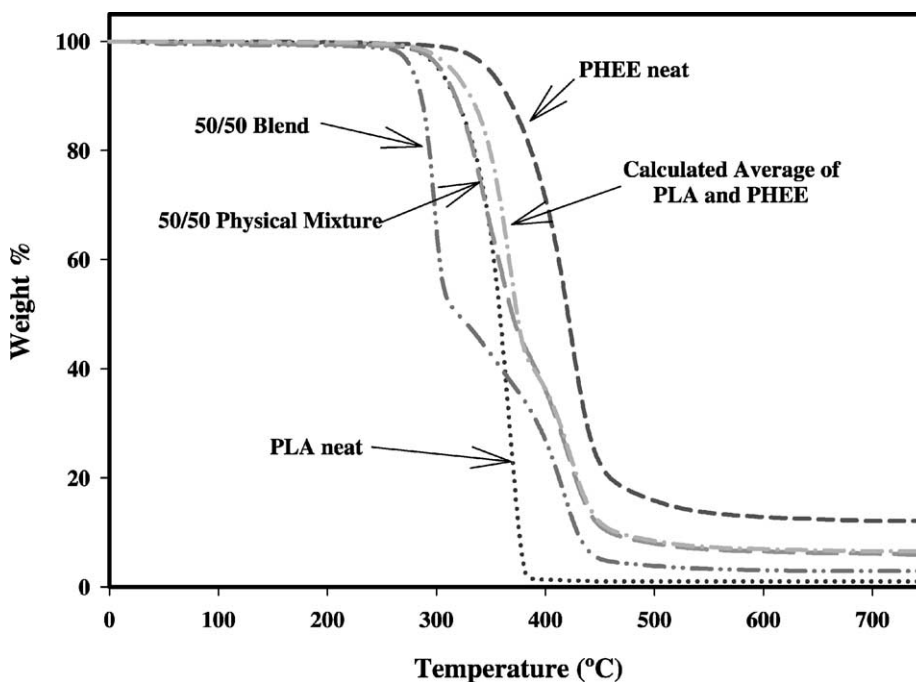


Fig. 10. Non-isothermal TGA tests on neat PLA, neat PHEE, 50/50 PLA/PHEE blend, and a physical mixture of equal amounts of the two neat polymers. A composed curve calculated from the average values of neat PLA and PHEE is also shown.

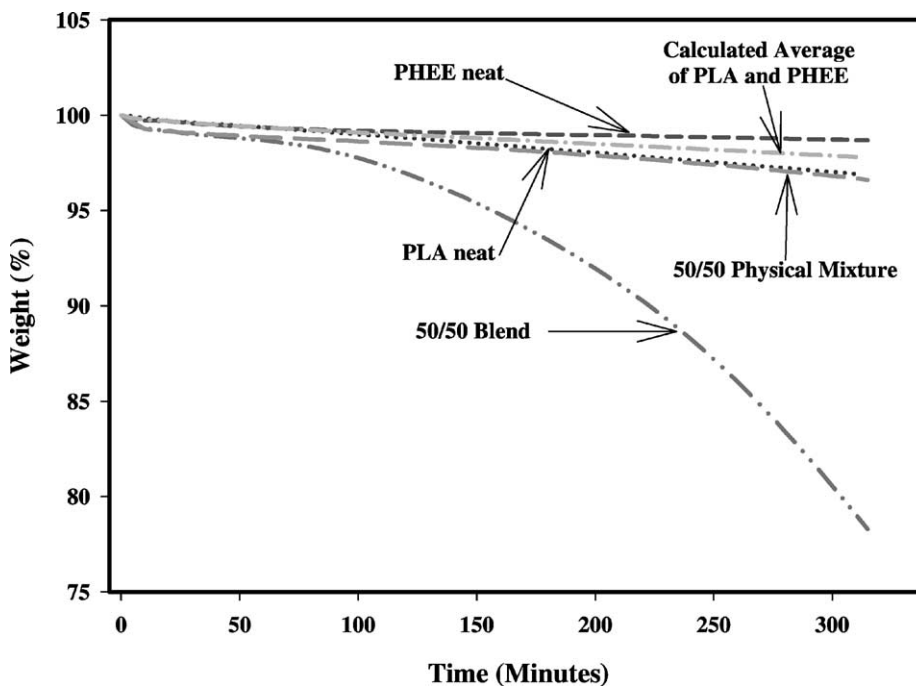


Fig. 11. Isothermal (200°C) TGA tests on neat PLA, neat PHEE, 50/50 PLA/PHEE blend, and a physical mixture of equal amounts of the two neat polymers. A composed curve calculated from the average values of neat PLA and PHEE is also shown.

in the batch mixer, is more than a simple physical blend of the two neat polymers consistent with the hydrogen bonding reported in our FTIR study [3].

#### 4. Conclusion

The DSC thermograms (second heating) of PLA/PHEE blends, prepared by melt blending, show two distinguishable  $T_g$  values as well as crystallization and melting enthalpies, corresponding to the  $T_g$  values of the two neat polymers, and the crystallization and melting enthalpies of neat PLA, respectively. Such thermograms have traditionally been used as direct evidence that the two polymers are not miscible. However, our DSC cycling procedure shows that the  $T_g$  values, as well as the enthalpies, are dependent on the number of DSC cycles the blends to which the blends are subjected. Eventually the two  $T_g$  values merge into one single  $T_g$  and the enthalpies reach zero, i.e. PLA in the blends is no longer capable of recrystallizing, strongly suggesting that these two polymers are miscible.

Our results also indicate that it is possible for DSC thermogram to show two distinguishable  $T_g$  values even if the polymers are miscible and the blending is done using standard mixing/blending procedures. Conclusions about miscibility drawn from such DSC thermograms could be erroneous if the blends have not been mixed adequately. The most definitive way to study miscibility is to establish a phase diagram, which is often time consuming and difficult experimentally. Repeated DSC heating–cooling cycles can be used as an easy check in such situations.

These results indicate that by changing blending/post-blending treatment conditions, different degrees of mixing of PLA and PHEE can be achieved, suggesting that biodegradable PLA/PHEE blends of controlled mechanical, thermal and optical properties may be obtained.

#### Acknowledgements

This research was conducted under CRADA number 58-3K95-8-0632 between the Agricultural Research Service and Biotechnology Research and Development Corporation. The superb technical work of B. Ahlgren is gratefully acknowledged. The authors also thank S. Mayes, P. Smith, M. Hairston and S. Todd for their technical support.

#### References

- [1] X. Cao, S.H. Gordon, J.L. Willett, D.J. Sessa, *Polym. Prepr.* 42 (1) (2001) 652–653.
- [2] J.L. Willett, W. Doane, US Patent 6,191,196 (2001).
- [3] X. Cao, S.H. Gordon, J.L. Willett, D.J. Sessa, *Polym. Prepr.* 42 (2) (2001) 623–624.
- [4] X. Cao, D.J. Sessa, W.J. Wolf, J.L. Willett, *J. Appl. Polym. Sci.* 80 (2001) 1737–1745.
- [5] D.R. Witzke, Ph.D. thesis, Michigan State University, 1997.
- [6] E.W. Fischer, H.J. Sterzel, G. Wegner, *Kolloid Z.: Z. Polym.* 251 (1973) 980.
- [7] M.N. Mang, J.E. White, A.P. Haag, S.L. Kram, C.N. Brown, *Polym. Prepr.* 36 (2) (1995) 180–181.
- [8] M. Gordon, J.S. Taylor, *J. Appl. Chem.* 2 (1952) 493–500.
- [9] G. Belorgey, R.E. Prud'Homme, *J. Polym. Sci., Polym. Phys.* 20 (1982) 191.
- [10] T.K. Kwei, E.M. Pearce, J.R. Pennacchia, M. Charton, *Macromolecules* 20 (5) (1987) 1174–1176.
- [11] R. Myers, Wyatt Technology Corporation, Santa Barbara, CA, private communication.